Hybrid electrokinetics for separation, mixing, and concentration of colloidal particles

Mandy L Y Sin[1]**, Yusuke Shimabukuro**[1] **and Pak Kin Wong**[1,2,3]

[1] Department of Aerospace and Mechanical Engineering, University of Arizona, Tucson, AZ, USA

[2] Biomedical Engineering Interdisciplinary Program and Bio5 Institute, University of Arizona, Tucson, AZ, USA

E-mail: pak@email.arizona.edu

Abstract

The advent of nanotechnology has facilitated the preparation of colloidal particles with adjustable sizes and the control of their size-dependent properties. Physical manipulation, such as separation, mixing, and concentration, of these colloidal particles represents an essential step for fully utilizing their potential in a wide spectrum of nanotechnology applications. In this study, we investigate hybrid electrokinetics, the combination of dielectrophoresis and electrohydrodynamics, for active manipulation of colloidal particles ranging from nanometers to micrometers in size. A concentric electrode configuration, which is optimized for generating electrohydrodynamic flow, has been designed to elucidate the effectiveness of hybrid electrokinetics and define the operating regimes for different microfluidic operations. The results indicate that the relative importance of electrohydrodynamics increases with decreasing particle size as predicted by a scaling analysis and that electrohydrodynamics is pivotal for manipulating nanoscale particles. Using the concentric electrodes, we demonstrate separation, mixing, and concentration of colloidal particles by adjusting the relative strengths of different electrokinetic phenomena. The effectiveness of hybrid electrokinetics indicates its potential to serve as a generic technique for active manipulation of colloidal particles in various nanotechnology applications.

S Supplementary data are available from stacks.iop.org/Nano/20/165701

(Some figures in this article are in colour only in the electronic version)

1. Introduction

Colloidal particles are the functional building blocks in nanotechnology and have attracted intense interest in numerous engineering and scientific applications, such as nanophotonics, energy harvesting, imaging, and diagnostics [1–6]. This is in part due to their controllable sizes and associated size-dependent properties, which can be tailored for various innovative applications. For instance, a laser-coupled opto-plasmonic tweezers (OPT) has been demonstrated using assembled colloidal particles coated with a gold thin film or different sized gold nanoparticles [7, 8]. The coupling efficiency of the OPT can be tuned by adjusting the size of the particles. Furthermore, colloidal quantum dots of different sizes have created pathways for creating sub-diffraction waveguides [9, 10] and obtaining desirable photoelectrochemical response and photoconversion efficiency for solar cell application [11, 12]. On the other hand, the size-tunable electrochemical and optical properties of colloidal particles have been demonstrated in numerous biological applications, especially in molecular diagnostics and imaging [13–16].

The wide applications of colloidal particles in nanotechnology warrant effective approaches for physical manipulation,

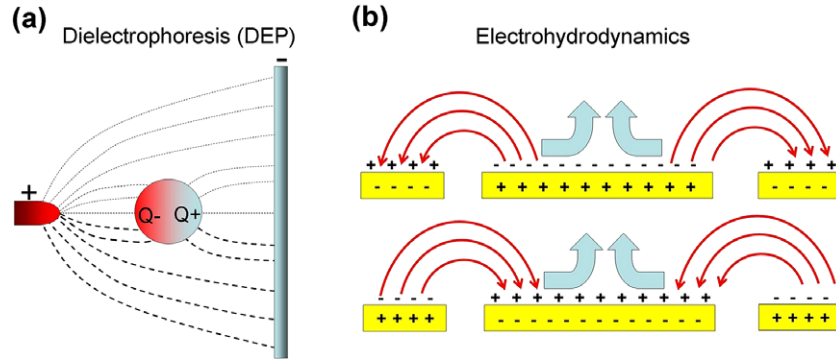[3] Address for correspondence: 1130 N. Mountain Avenue, Tucson, AZ, 85721, USA.

Figure 1. Principles of (a) dielectrophoresis and (b) AC electroosmosis.

such as separation, mixing, and concentration, of these particles. One of the approaches for active manipulation of colloidal particles, especially in microscale devices, is AC electrokinetics as these techniques are effective at small scale. For instance, dielectrophoresis (DEP) is one of the most well-known electrokinetic phenomena for manipulation of colloidal particles [17]. DEP describes the force experienced by a polarizable particle, in which a dipole is induced, under diverging AC electric fields. Under these conditions, the induced dipole experiences a net force and moves toward the high electric field region (positive DEP) or the low electric field region (negative DEP) depending on the effective polarization (figure 1(a)). The time average DEP force experienced by a spherical colloidal particle is given by [17, 18]

$$F_{\text{DEP}} = 2\pi R^3 \varepsilon_{\text{m}} \text{Re}[K(\omega)] \nabla |E_{\text{rms}}|^2 \qquad (1)$$

$$K(\omega) = \frac{\varepsilon_{\text{p}}^* - \varepsilon_{\text{m}}^*}{\varepsilon_{\text{p}}^* + 2\varepsilon_{\text{m}}^*} \qquad (2)$$

where R is the radius of the colloidal particle, ε_{m} is the permittivity of the medium, E_{rms} is the root mean square electric field, and $K(\omega)$ is the Clausius–Mossotti factor, which describes the effective polarization of the colloidal particle. ε_{p}^* and ε_{m}^* are the complex permittivity of the particle and the fluid medium. For homogeneous particles, the effective polarization is typically assumed to be dominated by interfacial polarization (Maxwell–Wagner polarization or space charge polarization) and the complex dielectric constants can be modeled as $\varepsilon_{\text{p,m}}^* = \varepsilon_{\text{p,m}} + \frac{\sigma_{\text{p,m}}}{j\omega}$. These relationships predict that the DEP force has a strong size dependence ($F_{\text{DEP}} \sim R^3$) and that the force is approximately constant when the applied frequency is below a crossover frequency (which is on the order of MHz) [18].

AC electroosmosis (ACEO) is another electrokinetic phenomenon that occurs at low frequencies (typically below 1 MHz), which is the bulk fluid motion induced by the electric field. It is known as a surface-driven bulk fluid motion and is a result of the interaction of the tangential electric field and the electrical double layer induced by the electric field on the electrode surface (figure 1(b)). For a parallel electrode configuration, the ACEO velocity v has been modeled using a linear double-layer approximation [19, 20].

$$\langle v(r) \rangle = \frac{1}{8} \frac{\varepsilon V_0^2 \Omega^2}{\mu r (1 + \Omega^2)^2} \qquad (3)$$

where ε is the fluid permittivity, V_0 is the amplitude of the AC potential, μ is the viscosity of the electrolyte, and r is the distance from the center of the electrode gap for a parallel electrode. The non-dimensional frequency Ω is given by

$$\Omega = \omega r \frac{\varepsilon}{\sigma} \frac{\pi}{2} \kappa \qquad (4)$$

where ω is the angular frequency of the applied electric field, σ is the conductivity of the medium, and κ is the reciprocal Debye length of the electrical double layer. This indicates that the ACEO flow increases with the second power of the applied voltage, similar to DEP [19].

Manipulations of micrometer and sub-micrometer particles using AC electrokinetics have been previously described [2, 5, 21, 22]. Nevertheless, the size dependence has not been studied systematically and the potential of combining multiple electrokinetic phenomena requires further investigation in order to fully understand the limitation and applicability of this approach. With a unique design of a concentric electrode configuration, which is optimized for generating ACEO flow [23, 24], we explore hybrid electrokinetics for the manipulation of colloidal particle ranging from 20 nm to 2 μm. The dynamic behaviors of these colloidal particles are investigated as a function of frequency from 80 Hz to 1 MHz. Since these electrokinetic phenomena have distinctive frequency dependences, it is possible to dynamically adjust the strengths of each force for a given size of particle. On the other hand, both forces are proportional to the second power of the applied voltage. In addition, we define the operating regimes and demonstrate separation, mixing, and concentration of colloidal particles, which are the three most fundamental microfluidic operations, using the same concentric electrode design. The implications of hybrid electrokinetics for the manipulation of nanoparticles are discussed.

2. Materials and methods

2.1. Creation of hybrid electrokinetic devices

The concentric electrode design used in this study consisted of a circular inner electrode and a concentric outer electrode surrounding the inner electrode. The diameter of the outer

electrode was 550 μm and the diameter of the inner electrode was 350 μm. The electrode arrays were microfabricated by evaporating 500 nm gold on a glass substrate with a 50 nm chromium adhesion layer and patterned by lift-off. For separation and concentration experiments, spacers of 170 μm in height were placed on both sides of the electrode and a microliter droplet of solution was put on top of the electrode before a microchamber was created by covering it with a cover slip. For the mixing experiment, T-shape microfluidic channels with two inlets and one outlet were fabricated using a combination of laser-machining and a two-step polymer molding process. The channel patterns were first laser-engraved on an acrylic plate with a 30 W CO_2 laser-machining system (Universal Laser Systems Inc.). Then, a master was obtained by urethane molding with the acrylic plate at 75 °C for ∼3 h. PDMS at a 10:1 base-to-curing agent ratio was then poured over the urethane master and cured at 75 °C for ∼3 h to create the T-shape PDMS microchannel. PDMS channels and the glass substrates with microelectrode arrays were sealed by plasma treatment using a low power plasma chamber (Harrick, model PDC-001). A digital syringe pump was used to introduce two fluid streams into the channel with the same pumping speed of 30 μl min^{-1}. Two fluid streams were DI water and DI water seeded with 20 nm red fluorescent particles (Invitrogen, F8786).

2.2. Colloidal particles and bacteria

Red fluorescent spheres of 20 nm, 200 nm, and 2 μm (Invitrogen, F8786, F8810, F8826) with excitation and emission peaks at 580 nm and 605 nm respectively were used in the experiment. The particles were diluted with DI water and adjusted to a conductivity of 0.3 mS m^{-1}. In this condition, we did not observe aggregation of the particles before the application of the electrical signal. For the separation experiment, yellow–green fluorescent spheres of 200 nm (Invitrogen, F8811) with fluorescence excitation and emission peaks at 505 and 515 nm were pre-mixed with 20 nm or 2 μm particles (red) before the experiment. For the concentration experiment, *E. coli* bacteria cultured in LB medium were directly loaded onto the device without further processing. The conductivity was 0.2 S m^{-1}.

2.3. Experimental setup

The electrokinetic device was mounted on a digital fluorescence microscope (Leica, DMI 4000B). The dynamics of particles were recorded by a CCD camera (Planetary Imaging, DMK 31AF03) and digitized into a video capture system (Image Source, IC Capture 2.0). The AC signal was generated by a function generator (HP, 33120A) by connecting the inner electrode with the driving signal and the outer electrode to the ground. All experiments were performed at room temperature.

2.4. Data analysis

For the mixing experiment, videos were taken to estimate the mixing efficiency. To quantify the efficiency of mixing, a mixing index is defined as

$$\text{Mixing index} = 1 - \frac{\sigma}{\overline{I}} = 1 - \sqrt{\frac{1}{n-1}\sum_{i=1}^{n}\left(\frac{I_i - \overline{I}}{\overline{I}}\right)^2}$$

where $\overline{I}$ and σ are the mean and standard deviation of the fluorescence intensity. n is the total number of pixels. I_i is the intensity at pixel i. The data were normalized by mapping fully mixed and unmixed solutions to 1 and 0, respectively. For the separation experiment, images were taken with green (510–560 nm) and red (590–650 nm) emission filters separately and combined using MetaMorph imaging software. For the concentration experiment, the data represent the fluorescence intensity at the center after 1 min of electrokinetic concentration. The images and videos were processed by ImageJ and MATLAB. The optical system was calibrated to ensure linearity in the intensity range. Data are reported as mean ± standard deviation for at least three consecutive experiments.

3. Results and discussion

3.1. Hybrid electrokinetics of different sized particles

To elucidate the dynamics of colloidal particles at different conditions and explore the applicability of hybrid electrokinetics, we measured the behaviors of particles of 20 nm, 200 nm, and 2 μm in a range of frequencies from 80 Hz to 1 MHz with a 6 V$_{pp}$ (peak-to-peak voltage). Upon application of the electric field, the particles generally reach steady state within 20 s (see supplementary information (available at stacks.iop.org/Nano/20/165701) for real-time videos of the experiment). Figure 2 shows the behaviors of the colloidal particles at low frequency range (80–600 Hz) after 1 min. For 2 μm particles, we observed aggregation of the particles at the edges in this frequency range. For 200 and 20 nm particles, we observed two equilibrium locations, the centers and the edges of the electrodes, for the particles depending on the applied frequency. In 200–600 Hz, a significant amount of 200 nm particles were aggregated at both equilibrium locations while 20 nm particles were mainly observed at the center at the same frequency. At lower frequency (80–100 Hz), all particles were aggregated at the edges of the electrodes. Figure 3 shows the particle behavior at higher frequencies (1 kHz–1 MHz). The amount of colloidal particles being concentrated decreases at 1–5 kHz. Only a small amount of 20 nm particles were aggregated at the center while the amount of 200 nm particles decreases gradually as the frequency increases. At higher frequency (∼500 kHz), 200 nm particles were observed to be concentrated at the edges of the electrodes while 2 μm and 20 nm particles were not concentrated.

The experimental results can be explained by the relative significance of DEP and ACEO effects with different particle sizes. DEP is a particle force, which depends on the third power of the size of the objects ($F_{\text{DEP}} \sim R^3$) and the gradient of the electric field ($\sim\nabla|E_{\text{rms}}|^2$), which is maximized at the edge of the electrode. Therefore, DEP is sensitive to the dimensions of the colloidal particle being manipulated and
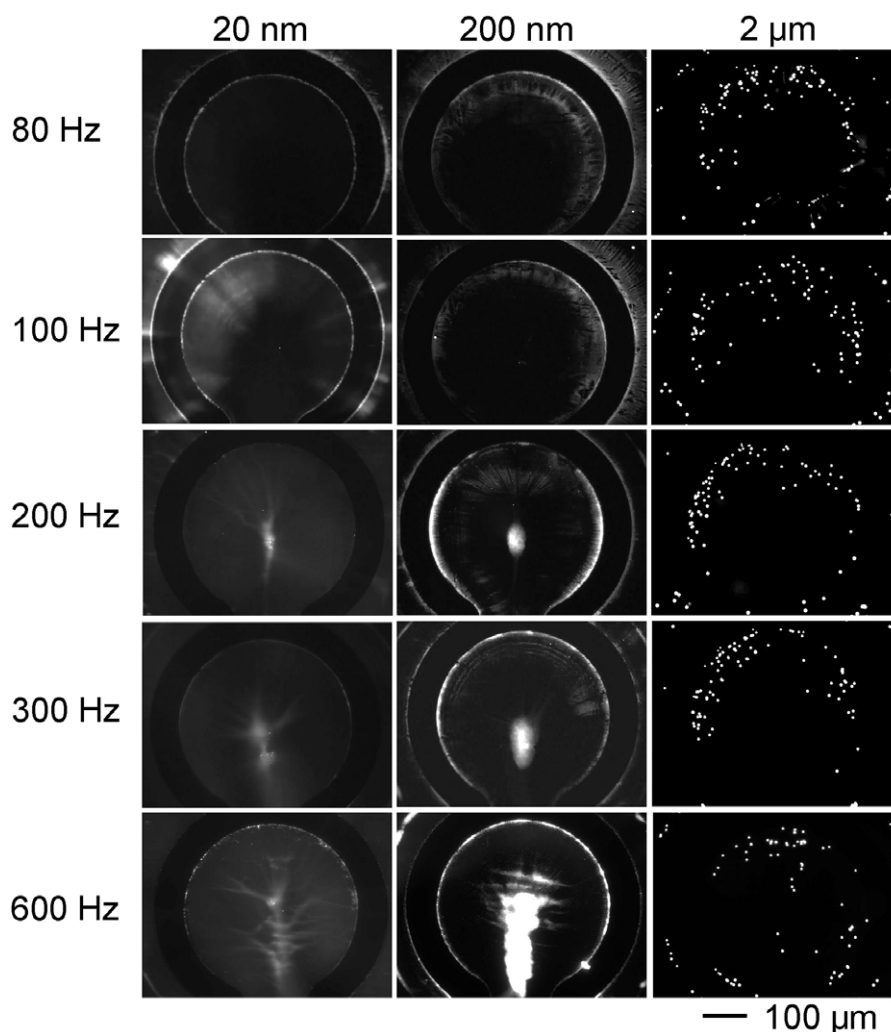
Figure 2. Electrokinetic manipulation of 20 nm, 200 nm, and 2 μm particles from 80 to 600 Hz. Fluorescence images represent the behavior of particles after the application of 6 V_{pp} at the corresponding frequency for 1 min.

particle aggregation at the edges indicates the dominance of DEP. On the other hand, ACEO is a bulk fluid force, which acts on the colloidal particles via hydrodynamic drag. At low Reynolds numbers, the hydrodynamic drag force scales linearly with the size of the objects and is proportional to the velocity of the particle through the fluid ($F_{ACEO} \sim F_{Drag} \sim R$). These predict a scaling dependence of the relative importance of DEP and ACEO for manipulating colloidal particles of different sizes $\frac{F_{ACEO}}{F_{DEP}} \sim \frac{R}{R^3} = R^{-2}$. While manipulation of colloidal particles is often considered to be contributed by DEP alone, the importance of electrohydrodynamics relative to DEP increases for small particles (e.g., nanoparticles). Particle aggregation at the center is considered to be the result of fluid motion induced by ACEO, which entrains the particles toward the stagnation point (i.e., the center of the inner electrode). Therefore, aggregations of 2 μm particles at the edges and 20 nm particles at the centers reflect the dominance of different forces for different sized particles under the same condition. For particles having an intermediate size (200 nm), aggregation was observed in both locations, indicating that both DEP and ACEO contribute to the observed behavior of

the particles. These results demonstrate a transition of the relative importance of DEP and ACEO for decreasing particle size, which is consistent with the scaling analysis that the importance of ACEO relative to DEP increases for decreasing particle size.

At lower frequency (80–100 Hz), particles were mainly aggregated at the edges for all sizes, which reflect the dominance of DEP, nevertheless, the long range electrohydrodynamic flow should still play an important role, which can be reflected by two observations. Firstly, there is a larger amount of particles aggregated at the edge of the inner electrode than the outer one because of the presence of the larger surface area in the inner electrode. Secondly, by applying the same electric field strength to parallel electrodes with a smaller surface area for generating ACEO (see supplementary information figure S2 available at stacks.iop.org/Nano/20/165701), we observed a much smaller amount of aggregation at the electrode edge. In our hybrid electrokinetic device, the concentric electrode design first generated long range fluid motion by ACEO, which entrained particles to the region near the electrode surface. The local
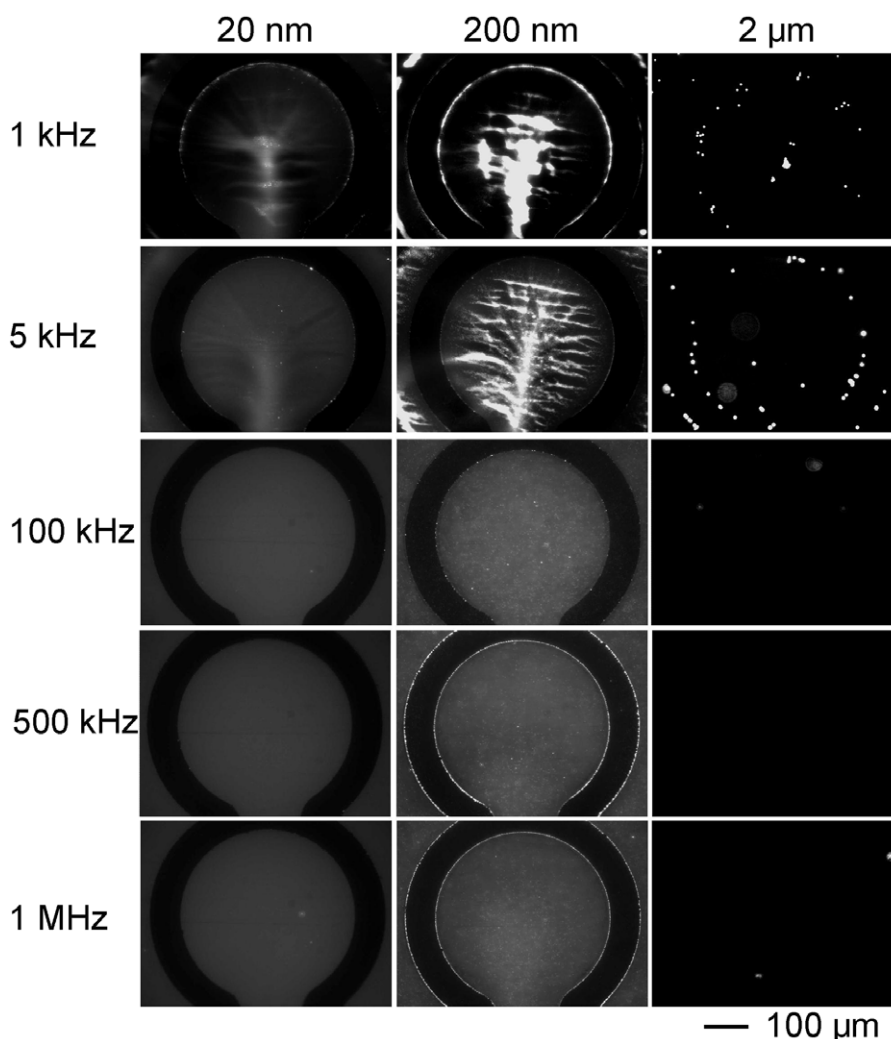
Figure 3. Electrokinetic manipulation of 20 nm, 200 nm, and 2 μm particles from 1 kHz to 1 MHz. Fluorescence images represent the behavior of particles after the application of 6 V_{pp} at the corresponding frequency for 1 min.

DEP force then allowed the particles to be collected onto the electrode surface. As a result, reduction of the surface area and the ACEO flow dramatically reduced the amount of particles trapped by DEP.

Figure 3 shows the particle behavior at higher frequency (1 kHz–1 MHz). The amount of colloidal particles being concentrated decreases at 1–5 kHz. Only a small amount of 20 nm particles were aggregated at the center while the amount 200 nm particles decrease gradually as the frequency increases. At higher frequency ($\sim$500 kHz), 200 nm particles were observed to be concentrated at the edges of the electrodes while 20 nm particles were not concentrated. The ACEO velocity decreases significantly as the frequency increases (see supplementary information figure S1 available at stacks.iop.org/Nano/20/165701), which is consistent with reported studies [20, 21, 25, 26]. The reduction of ACEO explains the reduced amount of particles being trapped at higher frequencies, since fluid motion is required to bring particles far way from the electrode to the electrode surface, where DEP is strongest for trapping the particles. These observations further supported the effectiveness of hybrid electrokinetics for the manipulation of colloidal particles of different sizes.

3.2. Electrokinetic separation of colloidal particles

Many interesting properties of colloidal particles are size-dependent; as a result, physical separation of colloidal particles is fundamentally important for various biosensing and nanotechnology applications. As observed in the frequency dependence study, particles of different sizes have distinct equilibrium positions at different frequencies. This creates a pathway for physically separating particles of different sizes using a combination of DEP and electrohydrodynamic flow (figures 4(a), (b)). To explore this possibility, yellow–green fluorescent particles of 200 nm and red fluorescent particles of 2 μm were mixed. At 3 kHz and 8 V_{pp}, the ACEO flow dragged 200 nm particles (green) toward the center of the electrode while DEP trapped 2 μm particles (red) at the edges of the electrode (figure 4(c)). This demonstrated physical separation of micrometer-sized and sub-micrometer-sized particles using our devices. By tuning the relative strength of the DEP force
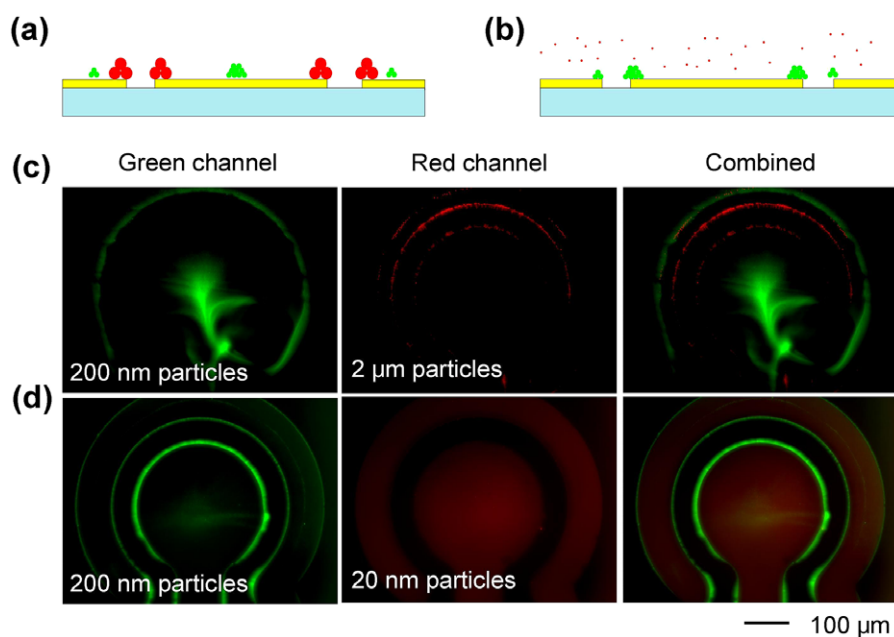
Figure 4. Electrokinetic separation. (a) Schematic for separating 200 nm particles (green) from 2 μm particles (red). Dielectrophoretic force dominates for large particles and traps them at the electrode edge while 200 nm particles are pushed toward the center of the electrode. (b) Schematic for separating 200 nm particles (green) from 20 nm particles (red). At an appropriate frequency, dielectrophoretic force is adequate for trapping 200 nm particles but not for trapping 20 nm particles. (c) Separation of 200 nm particles (green) from 2 μm particles (red) at 8 V_{pp} and 3 kHz. (d) Separation of 200 nm particles (green) from 20 nm particles (red) at 7 V_{pp} and 1 MHz.

and the hydrodynamic drag force generated by ACEO with varying frequencies, the same electrode configuration was also able to separate 20 and 200 nm particles. At 1 MHz and 7 V_{pp}, 200 nm particles (green) were trapped at the edge of the electrode while 20 nm particles (red) did not show observable changes in this condition (figure 4(d)).

3.3. Electrokinetic mixing of colloidal particles

Diffusion is the rate-limiting step in most microfluidic based biochemical analysis processes and the detection kinetics of many biosensors is limited by the mixing efficiency. Since colloidal particles have been applied in various biosensing applications, mixing of these particles could significantly enhance the performance of colloidal particles based biosensors in microfluidic devices. Our concentric electrode configuration combined with ACEO-induced vortices could be applied to enhance mixing of colloidal particles. Using the concentric electrode design, ACEO-induced fluid circulation can be generated for mixing colloidal particles. Figure 5(a) shows the principles of electrokinetic mixing using the concentric electrode. At an appropriate frequency for ACEO, a strong force (yellow and bigger arrows at the upper part of the electrode) is generated between the inner and outer electrodes and pushes the fluid toward the center of the electrode. At the opening region of the reference electrode, the force is relatively weak (red and smaller arrows at the lower part of the electrode). Imbalance of the forces generates ACEO-induced vortices (black arrows) over the electrode surface. Figure 5(b) shows the experimental setup in which the concentric electrode was integrated with

a T-shaped fluidic channel. Two streams of fluids were introduced into the channel with a digital syringe pump. A clear interface between the two fluid streams was observed due to the lack of effective mixing in the channel at this Reynolds number (less than 1). Video frames at 0 and 10 s showed the mixing enhancement with ACEO-induced vortices (figure 5(c)). A video of the electrokinetic mixing experiment is also available in the supplementary information (available at stacks.iop.org/Nano/20/165701). To quantify the mixing efficiency, a mixing index, which describes the uniformity of the solution of the electrode surface, is defined (see materials and methods). Fully mixed and non-mixed solutions are mapped to 1 and 0, respectively. In the experiment, over 90% mixing efficiency was obtained within 10 s, while diffusion based mixing required over 6 min for archiving a similar mixing efficiency (figure 5(d)).

3.4. Electrokinetic concentration of colloidal particles and bacteria

Electrokinetic concentration could potentially improve the sensitivity of particle based sensing. While DEP has been applied for the concentration of various micrometer-sized and sub-micrometer-sized objects, electrokinetic manipulation of nanoscale objects in a large region remains a challenging task due to the strong size dependence of DEP and the rapid decay of the electric field gradient. As predicted by the scaling analysis, the relative importance of electrohydrodynamics increases for small particles and can provide a useful technique for concentrating nanoscale particles. Under appropriate conditions, the fluid circulation increases the concentration
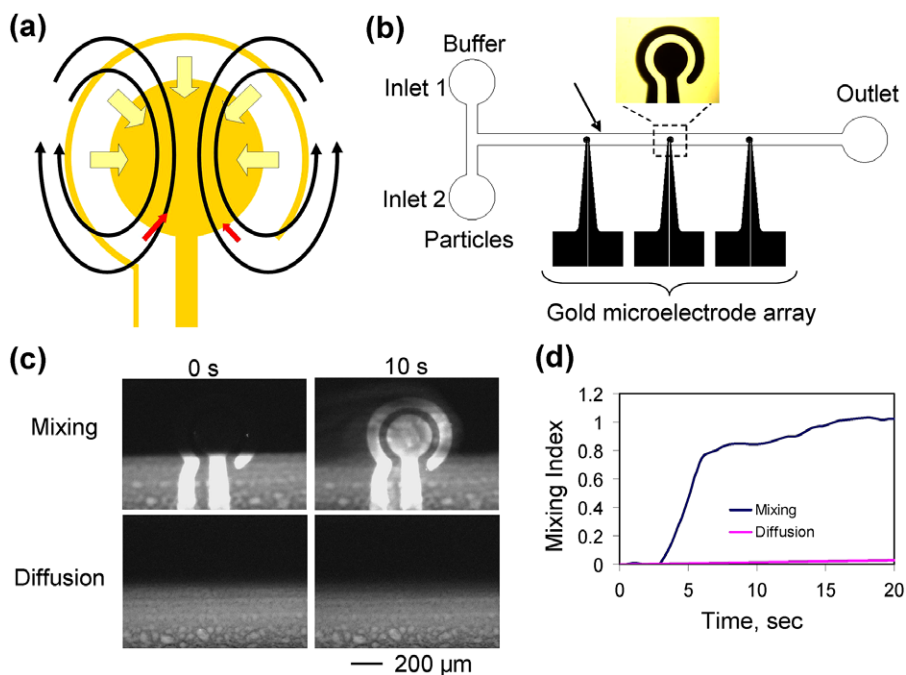
Figure 5. Electrokinetic mixing. (a) Schematic for particle mixing by electrokinetics. The opening of the outer electrode creates force imbalance and electrokinetic-induced vortices. (b) Experimental setup for mixing colloidal particles in a two-inlet microfluidic channel. (c) Fluorescence images of electrokinetic-induced mixing (top) and diffusion based mixing (bottom) at the beginning (left) and after 10 s (right). (d) Comparison of electrokinetic-induced mixing with diffusion based mixing.
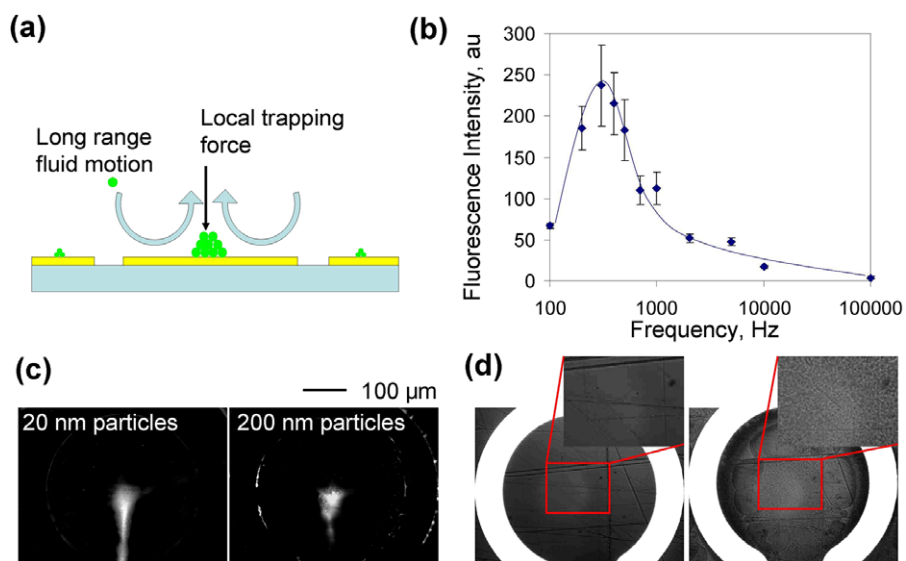

Figure 6. Electrokinetic concentration. (a) Schematic for particle concentration with hybrid electrokinetics. Long range fluid motion drives particles to regions near the electrode where other local electrokinetic forces trap the particles. (b) Frequency dependence of concentration of 200 nm particle at the center of the electrode. The concentration of particle can be increased over 100-fold. (c) Concentration 200 nm particles and 20 nm particles. (d) Concentration of *E. coli* on the electrode surface before (left) and after (right) the application of 3 V_{pp} and 10 kHz for 1 min.

efficiency by driving the colloidal particles far away toward the electrode where DEP is strongest (figure 6(a)). As shown in figure 6(b), we characterized the frequency dependence of the concentration process at 8 V_{pp} (peak-to-peak voltage) applied voltage. The concentration efficiency at the center of the electrode was maximized at an intermediate frequency, which was 300 Hz. At this frequency, the majority of the particles were pushed toward the center of the inner electrode and were concentrated into a small region on the order of approximately 35 μm in dimension. The concentration could be increased by over 100-fold within 1 min (figure 6(c)). Nanoscale particles were also concentrated effectively at the electrode edges at lower frequency ($\sim$80 Hz) (see figures 2 and 3). In addition, we demonstrated that the hybrid electrokinetic device was able

to concentrate *E. coil* bacteria on the electrode surface. Despite the large difference between the media, the behavior of *E. coli* was generally similar to that observed in the manipulation the colloidal particles. Since *E. coli* has a relatively large size ($\sim$2 μm), only a small voltage was required to trap them on the surface. At 3 V$_{pp}$ and 10 kHz, a large amount of bacteria were trapped on the electrode surface (figure 6(d)). This demonstrates the applicability of the devices for manipulating bioparticles.

3.5. Implication of hybrid electrokinetics in nanoparticles manipulation

Previously, Meinhart *et al* has demonstrated that the DEP force could have a significant influence on the measurement of electrohydrodynamic flow using micro particle image velocimetry (PIV) and a two-color PIV technique is required to eliminate the effect of DEP [23, 27]. This demonstrates that the effects of electrohydrodynamics and DEP can be comparable in the manipulation of colloidal particles. In the current study, we took advantage of the co-existence of different electrokinetic phenomena and systematically investigated their roles for manipulating colloidal particles with different sizes. Combining our concentric electrode design, our study demonstrated the effectiveness of hybrid electrokinetics for manipulation of nanoscale particles. Previously, DEP trapping of micro- and nanoscale particles was demonstrated [28–31]. In order to obtain adequate force for manipulating small particles in these studies, a large voltage and small electrodes (0.1–1 MV m^{-1}) were typically applied. While these designs allow trapping of the nanoparticles near the electrode, concentration of particles from a large region remains a challenging task due to the rapid decay of the electric field gradient. Our technique manipulates colloidal particles in a large region with electric field strengths on the order of 10 kV m^{-1}, which is 1–2 orders of magnitude smaller than a typical DEP concentrator for nanoscale objects [28, 29, 32, 33]. Several systems utilizing electrohydrodynamics have also been reported for manipulation of biological and nanoscale objects in the micrometers to nanometers range [23, 34–36]. Our study has systematically investigated the size dependence for the manipulation of colloidal particles with different sizes and provides general guidelines for optimizing the device design for future nanotechnology applications. This is the first demonstration of mixing, concentration, and separation of colloidal particles in the same device using AC electrokinetics.

An interesting observation in this study was the dominance of DEP at low frequency ($\sim$100 Hz). Under our experimental condition, the peak frequency of the ACEO velocity was below $\sim$100 Hz (as also supported by our data, see supplementary information figure S1 (available at stacks.iop.org/Nano/20/165701)). The ACEO velocity decreased monotonically as the applied frequency increased. One would expect ACEO dominated at low frequency. Nevertheless, we observed that particles were trapped at the edges at $\sim$100 Hz; this indicated DEP was stronger compared to the drag force induced by ACEO at low frequency. A likely explanation is that the DEP force is stronger at this range. For charged particles, a low frequency dielectric relaxation originated from the polarization of counterions in the electrical double layer has been reported [37, 38]. The low frequency dielectric relaxation plays an important role in the manipulation of nanoscale objects and is presumably responsible for the strong DEP force observed for biomolecules [39–42] and in our experiment.

4. Conclusions

In the study, a concentric electrode design has been demonstrated for active manipulation of colloidal particles from 20 nm to 2 μm in size by using a combination of DEP and electrohydrodynamics. The scaling dependence of the relative importance of DEP and electrohydrodynamics shows that the manipulation of larger and smaller particles is mainly contributed by DEP and electrohydrodynamics respectively. Therefore, by adjusting the relative strengths of these forces, separation, mixing, and concentration can be achieved using the same electrode design. Our study also demonstrated the importance of electrohydrodynamics for the concentration of nanoscale particles at the electrode edge, which is expected to be dominated by the DEP effect, by comparing the amount of particles aggregated at the edge of the concentric electrode with a larger surface area and the parallel electrodes with smaller surface area. This study forms the foundations for creating electrokinetic based biochemical processors, where all the microfluidic operations can be performed directly on the same electrode surface.

References

[1] Rosi N L and Mirkin C A 2005 Nanostructures in biodiagnostics *Chem. Rev.* **105** 1547–62
[2] Wong P K, Wang T H, Deval J H and Ho C M 2004 Electrokinetics in micro devices for biotechnology applications *IEEE–ASME Trans. Mechatron.* **9** 366–76
[3] Wong P K and Ho D 2008 Emergent diagnostic and therapeutic platforms for nanoengineered medicine *IEEE Nanotechnol. Mag.* **2** 9–13
[4] Park K 2007 Nanotechnology: what it can do for drug delivery *J. Controll. Release* **120** 1–3
[5] Hughes M P 2000 AC electrokinetics: applications for nanotechnology *Nanotechnology* **11** 124–32
[6] Hsiao V K S, Zheng Y B, Juluri B K and Huang T J 2008 Light-driven plasmonic switches based on au nanodisk arrays and photoresponsive liquid crystals *Adv. Mater.* **20** 3528–32
[7] Miao X and Lin L Y 2007 Large dielectrophoresis force and torque induced by localized surface plasmon resonance of Au nanoparticle array *Opt. Lett.* **32** 295–7

[8] Miao X Y, Wilson B K, Pun S H and Lin L Y 2008 Optical manipulation of micron/submicron sized particles and biomolecules through plasmonics *Opt. Express* **16** 13517–25

[9] Wang C J, Huang L, Parviz B A and Lin L Y 2006 Subdiffraction photon guidance by quantum-dot cascades *Nano Lett.* **6** 2549–53

[10] Huang L D, Wang C J and Lin L Y 2007 Comparison of cross-talk effects between colloidal quantum dot and conventional waveguides *Opt. Lett.* **32** 235–7

[11] Oregan B and Gratzel M 1991 A low-cost, high-efficiency solar-cell based on dye-sensitized colloidal TiO$_2$ films *Nature* **353** 737–40

[12] Kongkanand A, Tvrdy K, Takechi K, Kuno M and Kamat P V 2008 Quantum dot solar cells. tuning photoresponse through size and shape control of CdSe–TiO$_2$ architecture *J. Am. Chem. Soc.* **130** 4007–15

[13] Mirkin C A, Letsinger R L, Mucic R C and Storhoff J J 1996 A dna-based method for rationally assembling nanoparticles into macroscopic materials *Nature* **382** 607–9

[14] Lucas L J, Chesler J N and Yoon J Y 2007 Lab-on-a-chip immunoassay for multiple antibodies using microsphere light scattering and quantum dot emission *Biosensors Bioelectron.* **23** 675–81

[15] Han M Y, Gao X H, Su J Z and Nie S 2001 Quantum-dot-tagged microbeads for multiplexed optical coding of biomolecules *Nat. Biotechnol.* **19** 631–5

[16] Dulkeith E, Morteani A C, Niedereichholz T, Klar T A, Feldmann J, Levi S A, van Veggel F C J M, Reinhoudt D N, Moller M and Gittins D I 2002 Fluorescence quenching of dye molecules near gold nanoparticles: radiative and nonradiative effects *Phys. Rev. Lett.* **89** 2030021

[17] Pohl H A 1978 *Dielectrophoresis: The Behavior of Neutral Matter in Nonuniform Electric Fields* (Cambridge: Cambridge University Press)

[18] Jones T B 1995 *Electromechanics of Particles* (Cambridge: Cambridge University Press)

[19] Ramos A, Morgan H, Green N G and Castellanos A 1999 AC electric-field-induced fluid flow in microelectrodes *J. Colloid Interface Sci.* **217** 420–2

[20] Gonzalez A, Ramos A, Green N G, Castellanos A and Morgan H 2000 Fluid flow induced by nonuniform ac electric fields in electrolytes on microelectrodes. II. A linear double-layer analysis *Phys. Rev.* E **61** 4019–28

[21] Ramos A, Morgan H, Green N G and Castellanos A 1998 Ac electrokinetics: a review of forces in microelectrode structures *J. Phys. D: Appl. Phys.* **31** 2338–53

[22] Wu J, Ben Y X, Battigelli D and Chang H C 2005 Long-range ac electroosmotic trapping and detection of bioparticles *Ind. Eng. Chem. Res.* **44** 2815–22

[23] Bown M R and Meinhart C D 2006 AC electroosmotic flow in a DNA concentrator *Microfluid. Nanofluid.* **2** 513–23

[24] Wong P K, Chen C Y, Wang T H and Ho C M 2004 Electrokinetic bioprocessor for concentrating cells and molecules *Anal. Chem.* **76** 6908–14

[25] Green N G, Ramos A, Gonzalez A, Morgan H and Castellanos A 2002 Fluid flow induced by nonuniform ac electric fields in electrolytes on microelectrodes. III. Observation of streamlines and numerical simulation *Phys. Rev.* E **66** 026305

[26] Green N G, Ramos A, Gonzalez A, Morgan H and Castellanos A 2000 Fluid flow induced by nonuniform ac electric fields in electrolytes on microelectrodes. I. Experimental measurements *Phys. Rev.* E **61** 4011–8

[27] Meinhart C, Wang D Z and Turner K 2003 Measurement of ac electrokinetic flows *Biomed. Microdevices* **5** 139–45

[28] Lumsdon S O and Scott D M 2005 Assembly of colloidal particles into microwires using an alternating electric field *Langmuir* **21** 4874–80

[29] Zheng L F, Li S D, Brody J P and Burke P J 2004 Manipulating nanoparticles in solution with electrically contacted nanotubes using dielectrophoresis *Langmuir* **20** 8612–9

[30] Zheng L F, Brody J P and Burke P J 2004 Electronic manipulation of dna, proteins, and nanoparticles for potential circuit assembly *Biosensors Bioelectron.* **20** 606–19

[31] Kloepper K D, Onuta T D, Amarie D and Dragnea B 2004 Field-induced interfacial properties of gold nanoparticles in ac microelectrophoretic experiments *J. Phys. Chem.* B **108** 2547–53

[32] Hermanson K D, Lumsdon S O, Williams J P, Kaler E W and Velev O D 2001 Dielectrophoretic assembly of electrically functional microwires from nanoparticle suspensions *Science* **294** 1082–6

[33] Chan R H M, Fung C K M and Li W J 2004 Rapid assembly of carbon nanotubes for nanosensing by dielectrophoretic force *Nanotechnology* **15** S672–7

[34] Sasaki N, Kitamori T and Kim H B 2006 AC electroosmotic micromixer for chemical processing in a microchannel *Lab Chip* **6** 550–4

[35] Fatoyinbo H O, Hoettges K F, Reddy S M and Hughes M P 2007 An integrated dielectrophoretic quartz crystal microbalance (dep-qcm) device for rapid biosensing applications *Biosensors Bioelectron.* **23** 225–32

[36] Hoettges K F, McDonnell M B and Hughes M P 2003 Use of combined dielectrophoretic/electrohydrodynamic forces for biosensor enhancement *J. Phys. D: Appl. Phys.* **36** L101–4

[37] Schwarz G 1962 A theory of low-frequency dielectric dispersion of colloidal particles in electrolyte solution *J. Phys. Chem.* **66** 2636–42

[38] Okonski C T 1960 Electric properties of macromolecules. 5. Theory of ionic polarization in polyelectrolytes *J. Phys. Chem.* **64** 605–19

[39] Asbury C L and van den Engh G 1998 Trapping of DNA in nonuniform oscillating electric fields *Biophys. J.* **74** 1024–30

[40] Chou C F, Tegenfeldt J O, Bakajin O, Chan S S, Cox E C, Darnton N, Duke T and Austin R H 2002 Electrodeless dielectrophoresis of single- and double-stranded dna *Biophys. J.* **83** 2170–79

[41] Takashim S 1967 Effect of ions on dielectric relaxation of DNA *Biopolymers* **5** 899–913

[42] Washizu M, Suzuki S, Kurosawa O, Nishizaka T and Shinohara T 1994 Molecular dielectrophoresis of biopolymers *IEEE Trans. Ind. Appl.* **30** 835–43